Angewandte Chemie International Edition

DOI: 10.1002/anie.201101841

NMR Spectroscopy

Beyond the Silica Surface by Direct Silicon-29 Dynamic Nuclear Polarization**

Olivier Lafon,* Melanie Rosay, Fabien Aussenac, Xingyu Lu, Julien Trébosc, Odile Cristini, Christophe Kinowski, Nadia Touati, Hervé Vezin, and Jean-Paul Amoureux

Solid-state NMR spectroscopy is an irreplaceable technique for probing the atomic-level structure and dynamics in inorganic materials.[1] However, its applicability is plagued by a lack of sensitivity, which prevents the observation of interfaces, diluted species (defects, dopants), or isotopes, such as ^{29}Si, with low receptivities or long nuclear longitudinal relaxation times (T_{1n}).

Herein we show how direct ^{29}Si dynamic nuclear polarization (DNP) results in a 30-fold enhancement of ^{29}Si NMR signals from subsurface sites in porous silica, a material with applications in photonics, sensors, biomaterials, and catalysts.[2–4] The DNP method is based on the microwave-driven transfer of polarization from unpaired electrons to the nuclear spins. Originally introduced at low magnetic fields,[5] DNP was then applied under magic-angle spinning (MAS) and at high magnetic field to combine sensitivity and high resolution.[6–11] The extension of high-field MAS DNP to inorganic materials faces three challenges: 1) the incorporation of paramagnetic agents in materials, 2) the distribution of polarization throughout nonprotonated samples for which ^{1}H–^{1}H spin diffusion cannot be used, and 3) the observation of isotopes other than ^{13}C or ^{15}N.[12]

We show herein how these challenges can be handled in the case of porous silica used in photonics (see Figure S1 in the Supporting Information).[2] The mean pore diameter of these samples is about 75 Å, and radicals such 4-amino-(2,2,6,6-tetramethylpiperidin-1-yloxyl)(4-amino-TEMPO) or 1-(TEMPO-4-oxy)-3-(TEMPO-4-amino)propan-2-ol (TOTAPOL)[13] were introduced by impregnation within the pores as the source of polarization for DNP.[14,15] A first possibility to enhance the ^{29}Si signal by DNP consists of the indirect polarization of ^{29}Si nuclei via ^{1}H using $^{1}H \rightarrow ^{29}Si$ cross-polarization (CP).[12] This method enhances the polarization of ^{29}Si nuclei located near the surface but not in the bulk, since 1) there are few protons inside the bulk silica xerogel[16] and 2) CP transfers are only effective up to a few angstroms and suffer from dipolar truncation.[17] As an alternative, we explore the direct DNP of ^{29}Si nuclei. This method has been tested, mainly at low magnetic field under static conditions, for amorphous or doped silicon containing endogenous paramagnetic centers.[18–22] Herein we demonstrate the efficiency of direct ^{29}Si MAS DNP for porous silica at high field.

Figure 1 shows how the direct DNP of ^{29}Si nuclei strongly increases the signal intensity of porous silica. The employed pulse sequence is displayed in Figure 1 a. Figure 1 b presents a comparison of one-dimensional (1D) natural-abundance ^{29}Si MAS NMR spectra obtained with and without microwave irradiation. For materials containing TOTAPOL in a concentration of $c_m = 15$ mM, we measured a DNP signal enhancement of $|\varepsilon| = 30$.

The direct DNP ^{29}Si NMR spectrum can be compared with that obtained by indirect DNP (see Figure 1 c). The signal enhancements of direct DNP are larger than those measured for indirect DNP ($\varepsilon_{CP} = 13$). However, for direct DNP, the polarization builds up within hundreds of seconds (see Table 1), whereas the time constant of polarization build-up for indirect DNP is a few seconds.[23] Under the experimental conditions of Figure 1 c, the sensitivity of indirect DNP is 35 % higher than that of direct DNP. In practice, direct DNP complements indirect DNP since, as seen in Figure 1 c, there are large differences between the direct and indirect

Table 1: Influence of TOTAPOL concentration on the direct polarization of ^{29}Si nuclei.

c_m [mM^{-1}]	$\lvert\varepsilon\rvert$ [a]	τ_f [s][b]	τ_s [s][b]	α [%][b]
7	29	190	2200	87
15	30	120	1200	81
30	20	110	1100	74

[a] The experimental conditions are those of Figure 1 b. [b] Parameters for the fit of intensity build-up curves with Equation (1).

---

[*] Dr. O. Lafon, X. Lu, Dr. J. Trébosc, Prof. J.-P. Amoureux
Unité de Catalyse et de Chimie du Solide (UCCS)
UMR CNRS 8181, École Nationale Supérieure de Chimie de Lille
University of Lille-Nord de France
Bât. C7, B.P. 90108, 59652 Villeneuve d'Ascq Cedex (France)
E-mail: olivier.lafon@ensc-lille.fr

Dr. M. Rosay
Bruker Biospin Corporation
15 Fortune Drive, Billerica, MA 01821 (USA)

Dr. F. Aussenac
Bruker Biospin SA
34, rue de l'Industrie, 67166 Wissembourg Cedex (France)

Dr. O. Cristini, Dr. C. Kinowski
Laboratoire de Physique des Lasers, Atomes et Molécules (Phlam)
CNRS-UMR 8523
Bât. P5 Université Lille 1-Sciences et Technologies
59655 Villeneuve d'Ascq Cedex (France)

N. Touati, Dr. H. Vezin
Laboratoire de Spectrochimie Infrarouge et Raman
UMR-CNRS 8516, Université des Sciences et Technologies de Lille
59655 Villeneuve d'Ascq cedex (France)

[**] We are grateful for funding provided by the Region Nord/Pas de Calais, Europe (FEDER), CNRS, French Minister of Science, FR-3050, USTL, ENSCL, Bruker BIOSPIN, and Contract No. ANR-2010-JCJC-0811-01.

Supporting information for this article is available on the WWW under http://dx.doi.org/10.1002/anie.201101841.

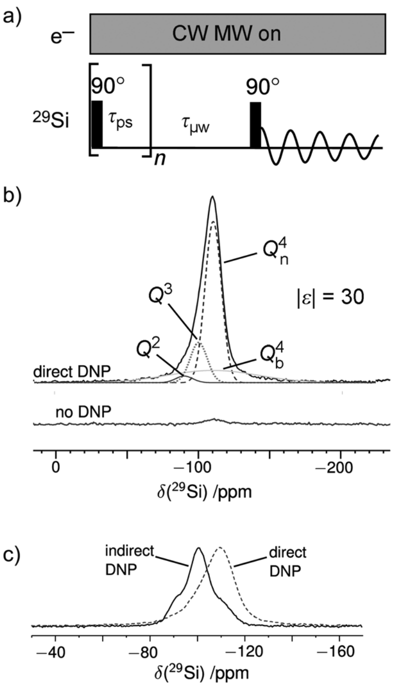

Figure 1. a) Pulse sequence used for 1D direct DNP MAS experiment. The equilibrium Boltzmann ^{29}Si polarization was eliminated by a presaturation, consisting of a train of $n = 100$ 90° pulses, separated by a time $\tau_{ps} = 0.3$ ms. The longitudinal ^{29}Si polarization builds up during the microwave polarization time $\tau_{\mu w}$. The same experiment without microwave irradiation serves as a reference for the measurement of signal enhancement ε by direct DNP. b) Natural-abundance ^{29}Si NMR spectra of porous silica with TOTAPOL ($c_m = 15$ mM) with (top) and without (bottom) direct ^{29}Si DNP. The deconvolution of the direct DNP spectrum is also displayed. Both spectra were acquired at a MAS frequency $\nu_r = 10$ kHz, a B^0 field position DNP(−) (see Figure 2), and $\tau_{\mu w} = 240$ s. Sample temperature was 98 K with microwave off. The NMR spectra shown here result from averaging 16 scans. c) Comparison between the natural-abundance ^{29}Si NMR spectra obtained with direct DNP (dashed line) and indirect DNP via ^{1}H (continuous line) for the same sample. The direct DNP spectrum is identical to that displayed in (b). The two spectra were scaled to the same maximum intensity. The deconvolution and experimental conditions for the indirect DNP spectrum are given in the Supporting Information.

DNP ^{29}Si signals. The direct DNP spectrum displays a maximum at $\delta = -110$ ppm, the chemical shift of (Si–O)$_4$Si (Q^4) sites.[16] Conversely, in the indirect DNP spectrum, we observe the largest intensity at $\delta = -100$ ppm, the δ value of (Si–O)$_3$Si(OH) (Q^3) sites, and a marked shoulder at $\delta = -90$ ppm, corresponding to (Si–O)$_2$Si(OH)$_2$ (Q^2) sites. In porous silica, the Q^2 and Q^3 sites cover the surface of the pores, whereas the Q^4 sites represent the bulk of silica network. We can conclude that the direct ^{29}Si DNP is able to polarize the subsurface Q^4 ^{29}Si nuclei, whereas indirect ^{29}Si DNP enhances the polarization of surface nuclei.

The direct DNP ^{29}Si signal has been fitted as the sum of four contributions, those of Q^2, Q^3, Q^4_n, and Q^4_b sites (the fit procedure is detailed in the Supporting Information). The Q^4_b contribution represents the signal arising from Q^4 sites located in the vicinity of paramagnetic centers and broadened by electron–nucleus interactions,[24] whereas the narrow Q^4_n contribution corresponds to the other Q^4 sites. The relative areas of Q^2, Q^3, Q^4_b, and Q^4_n contributions are 3, 17, 21, and 59 %, respectively, thus confirming the larger polarization of subsurface Q^4 sites.

The influence of nature and concentration of the radical on the efficiency of direct ^{29}Si DNP was investigated. For porous silica containing 30 mM 4-amino-TEMPO, the signal enhancement by direct ^{29}Si DNP was $|\varepsilon| = 11$, a threefold lower value than that obtained with 15 mM TOTAPOL. This result confirms that at high magnetic fields, biradicals benefit from the efficient cross-effect (CE) DNP mechanism.[13,15,25,26] The TOTAPOL concentration in porous silica was optimized, and the largest nuclear polarization was obtained for $c_m = 15$ mM. Furthermore, EPR measurements indicate that the c_m values reported in Table 1 are about 15 % higher than expected from full impregnation with the TOTAPOL solution (see the Supporting Information). This result suggests the existence of specific interactions between the TOTAPOL molecules and the silica surface.

Figure 2 shows the dependence of the DNP enhancement on the static magnetic field B^0. The low-field DNP enhancement is 30 % higher than that obtained at high field. These features are typical of direct DNP for isotopes with low gyromagnetic ratios when TOTAPOL is used as a polarizing agent and the CE is the polarization mechanism.[27,23] Direct DNP experiments were performed at the low-field extremum, and all ε values reported herein are negative. Conversely, indirect DNP experiments were performed at a high field position, resulting in positive ε_{CP} values.[23]

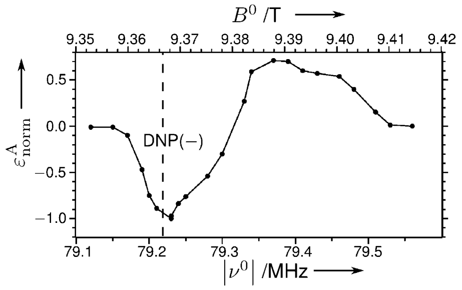

Figure 2. Dependence of normalized ^{29}Si DNP enhancement on the magnetic field B^0. The scale corresponding to ^{29}Si Larmor frequency $|\nu^0|$ is also displayed. The sample was porous silica impregnated with $c_m = 15$ mM TOTAPOL. The DNP enhancements are normalized according to $\varepsilon^A_{norm} = \varepsilon^A / |\varepsilon^A_{max}|$ where $|\varepsilon^A_{max}|$ is the absolute value of the maximal ^{29}Si DNP enhancement. The ε^A values for each B^0 magnitude were determined from the integrals of ^{29}Si peaks with and without microwave irradiation using $\tau_{\mu w} = 60$ s.

The dependences of direct ^{29}Si DNP enhancement on sample temperature T or MAS frequency ν_r are weaker than those reported for the indirect DNP of frozen solutions (see the Supporting Information). Besides, the build-up time of ^{29}Si signal intensity and integral do not depend on the value of ν_r (see Figure 3 a and Figure S4 in the Supporting Information).

Using a phenomenological approach, the normalized build-up curves of DNP-enhanced intensity at −110 ppm (Figure 3 a) were modeled as a bi-exponential function [Eq. (1)]:

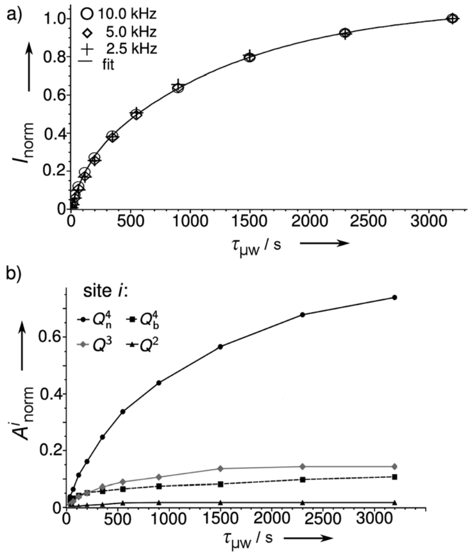

Figure 3. Build-up curves of ^{29}Si polarization for direct DNP experiments. a) Build-up curve of DNP-enhanced ^{29}Si signal intensity as a function of $\tau_{\mu w}$ delay for $\nu_r = 2.5$, 5.0, and 10.0 kHz. The sample was porous silica impregnated with $c_m = 15$ mM TOTAPOL. For each ν_r value, the DNP-enhanced ^{29}Si signal intensities $I(\tau_{\mu w})$ are normalized with respect to the signal intensities at $\tau_{\mu w} = 3200$ s: $I_{norm} = I(\tau_{\mu w})/I(3200)$. The $I(3200)$ intensity, which is the same at $\nu_r = 5.0$ and 10 kHz, is reduced by 10% at $\nu_r = 2.5$ kHz. b) Build-up curve of direct DNP-enhanced integrals of different ^{29}Si sites, $i = Q^2$, Q^3, Q^4_n, and Q^4_b, as a function of $\tau_{\mu w}$ delay. The DNP-enhanced integrals $A^i(\tau_{\mu w})$ for all ^{29}Si sites are obtained by deconvolution. Here, the $A^i(\tau_{\mu w})$ integrals are normalized with respect to the total integral over all ^{29}Si signals at $\tau_{\mu w} = 3200$ s: $A^i_{norm} = A^i(\tau_{\mu w})/A(3200)$.

$$I_{\mathrm{norm}}(\tau_{\mu\mathrm{w}}) = I^{\infty}\left\{(1-\alpha)\left[1-\exp\left(-\frac{\tau_{\mu\mathrm{w}}}{\tau_{\mathrm{f}}}\right)\right] + \alpha\left[1-\exp\left(-\frac{\tau_{\mu\mathrm{w}}}{\tau_{\mathrm{s}}}\right)\right]\right\} \tag{1}$$

where τ_f and τ_s represent the time constants of the fast and slow components, and α is the fractional contribution of the slow component to the DNP-enhanced ^{29}Si signal. The fast and slow components may be interpreted as arising from ^{29}Si nuclei close to or remote from TOTAPOL molecules, respectively, in a simple two-site model. For increasing c_m values, faster polarization build-up is observed, since each TOTAPOL molecule has to polarize a smaller volume (see Table 1). Besides, the size of the parameter α decreases with increasing c_m, since more molecules are located in the vicinity of a biradical.

We observed a line narrowing of the DNP-enhanced ^{29}Si signal for increasing $\tau_{\mu w}$ delay, stemming from the slower build-up of Q^4_n polarization compared to that of Q^4_b polarization (see Figure 3b and Figure S5 in the Supporting Information). This observation is consistent with TOTAPOL being closer to Q^4_b sites than to Q^4_n ones.

The role of ^{29}Si spin diffusion has been shown for direct ^{29}Si DNP of static samples at a few Kelvin,[21,22] but its involvement under MAS at approximately 100 K remains an open question. The spin diffusion coefficient D between ^{29}Si nuclei can be estimated using Equation (2):[28,10]

$$D = \bar{a}^2 \pi \bar{\nu}_d \tag{2}$$

where $\bar{\nu}_d$ is the average dipolar interaction (expressed in Hz) at a characteristic distance $\bar{a}$ between ^{29}Si isotopes. The derivations of $\bar{\nu}_d$ and $\bar{a}$ are given in the Supporting Information. The calculated D values at different MAS frequencies are reported in Table 2. From $\nu_r = 2.5$ to 10.0 kHz, the D coefficient decreases from 3.8 to 1.0 Å^{2}s^{-1}. These values are two orders of magnitude smaller than those obtained under static conditions in silicon.[21,22]

Table 2: Spin diffusion parameters for different MAS frequencies and $c_m = 15$ mM.

ν_r [kHz]	D [Å^2 s^{-1}][a]	T_{sd} [s][b]
2.5	3.8	150
5.0	1.9	300
10.0	1.0	600

[a] Calculated from Equation (2). [b] Calculated from Equation (3).

Using the estimated D coefficient, the spin diffusion time constant T_{sd} to transfer nuclear polarization through the half-distance $R/2$ between two TOTAPOL molecules is given by Equation (3):[22]

$$T_{\mathrm{sd}} = \frac{(R/2)^2}{D} \tag{3}$$

The average distance R in Å between two TOTAPOL molecules can be estimated from Equation (4):

$$R = (c_{\mathrm{m}}\, 10^{-30}\, N_{\mathrm{A}})^{-1/3} \tag{4}$$

where c_m is expressed in mM and N_A is the Avogadro number. For $c_m = 15$ mM, Equation (4) yields $R = 48$ Å. The T_{sd} values estimated from Equation (3) are reported in Table 2. Even at $\nu_r = 10$ kHz, the T_{sd} value is smaller than the τ_s time constant. Therefore, the limiting factor for the slow build-up of Q^4_n polarization is not the ^{29}Si spin diffusion but the slow direct polarization of ^{29}Si nuclei by CE transfer. This result explains why MAS frequency does not affect the polarization build-up curves (see Figure 3a and Figure S4 in the Supporting Information).

The estimate of the spin diffusion barrier radius r_d provides further evidence that the effect of ^{29}Si spin diffusion can be neglected in direct ^{29}Si DNP. For the investigated systems, the electron longitudinal relaxation times T_{1e} are shorter than the ^{29}Si transverse longitudinal relaxation times ($T_{1e} < T_{2n}$), and the radius r_d is given by Equation (5), Khutsishvili's definition:[29]

$$r_{\mathrm{d}} \approx \left[2S\frac{\gamma_{\mathrm{e}}}{\gamma(^{29}\mathrm{Si})}B_{\mathrm{S}}\left(\frac{S\hbar\gamma_{\mathrm{e}}B^0}{k_{\mathrm{B}}T}\right)\right]^{1/4}\bar{a} \tag{5}$$

where S is effective spin quantum number for the unpaired electron, γ_e and $\gamma(^{29}\mathrm{Si})$ are the gyromagnetic ratios of electron and ^{29}Si nucleus, B_S is the Brillouin function with parameter S, $\hbar$ the reduced Planck constant, $B^0 = 9.391$ T the static magnetic field, k_B the Boltzmann constant, $T = 98$ K the sample temperature. As TOTAPOL is a biradical, the spin S is equal to 1/2 or 1 depending on the strength and the type of couplings between the two unpaired electrons. Under the experimental conditions, Equation (5) yields radii r_d of about 35 Å for $S = 1/2$ and 45 Å for $S = 1$. These r_d values are larger than the $R/2$ value and the average pore wall thickness $\bar{h} = 15$ Å, which is estimated in the Supporting Information. Therefore, all ^{29}Si nuclei of the sample are core nuclei enclosed in the diffusion barrier, and the efficiency of ^{29}Si spin diffusion is reduced not only by MAS but also by significant differences in hyperfine shifts between two neighboring ^{29}Si nuclei.

In the absence of spin diffusion, the ^{29}Si nuclei can only be polarized if they are involved in a CE transfer, and the direct ^{29}Si DNP enhances the ^{29}Si nuclei with T_{1n} times governed by electron–^{29}Si interaction. Besides, the build-up time constant for CE transfer may be shorter than T_{1n}, but both time constants are of the same order of magnitude.[30] Hence, the slow polarization build-up of ^{29}Si nuclei is the consequence of the long ^{29}Si T_{1n} times.

In conclusion, we have shown that NMR signals of subsurface and surface ^{29}Si sites in porous materials can be dramatically enhanced by direct ^{29}Si MAS DNP at high B^0 field. Signal enhancements by a factor of 30 were measured and higher $|\varepsilon|$ values are expected using sapphire rotors instead of ZrO_2[9,31] or utilizing radicals displaying narrower EPR spectra than TOTAPOL.[27] This method supplements indirect DNP via ^{1}H, since it allows detection of subsurface atoms even for nonprotonated samples. This subsurface technique opens the way for the characterization of siliceous materials, such as glasses, catalysts or nanomaterials, by MAS DNP. Undoubtedly this approach will allow the detection of defects, impurities, and other sites inaccessible by surface-enhanced methods.

Experimental Section

Nanoporous silica with natural isotopic abundance was synthesized using the sol–gel process of hydrolysis and condensation of tetramethyl orthosilicate.[2] The ground xerogels were impregnated with 4-amino-TEMPO or TOTAPOL solutions in [$^2H_6$]-DMSO/^2H_2O/H_2O mixture (78:14:8 wt/wt/wt).

All solid-state DNP MAS experiments were performed on a commercial Bruker BioSpin Avance III DNP spectrometer operating at a microwave frequency of 263 GHz and a ^{29}Si frequency of 79.2 MHz.[9] The wide-bore 9.4 T NMR magnet was equipped with a double-resonance ^{1}H/X 3.2 mm low-temperature probe. The sample was placed in a 3.2 mm ZrO_2 rotor. The ^{29}Si NMR spectra enhanced by direct DNP were recorded using the pulse sequence displayed in Figure 1 a. Unless otherwise specified, the experimental parameters are those indicated in the caption of Figure 1 b.

Additional details about the experimental procedures are given in the Supporting Information.

Received: March 15, 2011
Revised: May 30, 2011

Keywords: dynamic nuclear polarization · mesoporous materials · NMR spectroscopy · silicon

---

[1] I. Farnan, H. Cho, W. J. Weber, *Nature* **2007**, *445*, 190.
[2] O. Robbe, K. Woznica, E. Berrier, G. Ehrhart, B. Capoen, M. Bouazaoui, S. Turrell, *Thin Solid Films* **2006**, *515*, 73.
[3] K. E. Shopsowitz, H. Qi, W. Y. Hamad, M. J. MacLachlan, *Nature* **2010**, *468*, 422.
[4] Z. Chen, Y. Jiang, D. R. Dunphy, D. P. Adams, C. Hodges, N. Liu, N. Zhang, G. Xomeritakis, X. Jin, N. R. Aluru, S. J. Gaik, H. W. Hillhouse, C. Jeffrey Brinker, *Nat. Mater.* **2010**, *9*, 667.
[5] T. R. Carver, C. P. Slichter, *Phys. Rev.* **1953**, *92*, 212.
[6] R. Wind, M. Duijvestijn, C. van der Lugt, A. Manenschijn, J. Vriend, *Prog. Nucl. Magn. Reson. Spectrosc.* **1985**, *17*, 33.
[7] L. R. Becerra, G. J. Gerfen, R. J. Temkin, D. J. Singel, R. G. Griffin, *Phys. Rev. Lett.* **1993**, *71*, 3561.
[8] D. A. Hall, D. C. Maus, G. J. Gerfen, S. J. Inati, L. R. Becerra, F. W. Dahlquist, R. G. Griffin, *Science* **1997**, *276*, 930.
[9] M. Rosay, L. Tometich, S. Pawsey, R. Bader, R. Schauwecker, M. Blank, P. M. Borchard, S. R. Cauffman, K. L. Felch, R. T. Weber, R. J. Temkin, R. G. Griffin, W. E. Maas, *Phys. Chem. Chem. Phys.* **2010**, *12*, 5850.
[10] P. C. A. van der Wel, K.-N. Hu, J. Lewandowski, R. G. Griffin, *J. Am. Chem. Soc.* **2006**, *128*, 10840.
[11] V. S. Bajaj, M. L. Mak-Jurkauskas, M. Belenky, J. Herzfeld, R. G. Griffin, *Proc. Natl. Acad. Sci. USA* **2009**, *106*, 9244.
[12] M. Lelli, D. Gajan, A. Lesage, M. A. Caporini, V. Vitzthum, P. Miéville, F. Héroguel, F. Rascón, A. Roussey, C. Thieuleux, M. Boualleg, L. Veyre, G. Bodenhausen, C. Copéret, L. Emsley, *J. Am. Chem. Soc.* **2011**, *133*, 2104.
[13] C. Song, K.-N. Hu, C.-G. Joo, T. M. Swager, R. G. Griffin, *J. Am. Chem. Soc.* **2006**, *128*, 11385.
[14] J.-P. Amoureux, O. Lafon, J. Trébosc, L. Delevoye, G. Tricot, L. Montagne, in *Honoris causa of Prof. Alex Pines*, June **2010**.
[15] A. Lesage, M. Lelli, D. Gajan, M. A. Caporini, V. Vitzthum, P. Miéville, J. Alauzun, A. Roussey, C. Thieuleux, A. Mehdi, G. Bodenhausen, C. Copéret, L. Emsley, *J. Am. Chem. Soc.* **2010**, *132*, 15459.
[16] I. S. Chuang, D. R. Kinney, G. E. Maciel, *J. Am. Chem. Soc.* **1993**, *115*, 8695.
[17] M. Hologne, P. Bertani, T. Azaïs, C. Bonhomme, J. Hirschinger, *Solid State Nucl. Magn. Reson.* **2005**, *28*, 50.
[18] A. Abragam, J. Combrisson, I. Solomon, *C. R. Hebd. Seances Acad. Sci.* **1958**, *246*, 1035.
[19] H. Lock, R. Wind, G. Maciel, N. Zumbulyadis, *Solid State Commun.* **1987**, *64*, 41.
[20] A. Henstra, P. Dirksen, W. T. Wenckebach, *Phys. Lett. A* **1988**, *134*, 134.
[21] A. E. Dementyev, D. G. Cory, C. Ramanathan, *Phys. Rev. Lett.* **2008**, *100*, 127601.
[22] H. Hayashi, K. M. Itoh, L. S. Vlasenko, *Phys. Rev. B* **2008**, *78*, 153201.
[23] T. Maly, A.-F. Miller, R. G. Griffin, *ChemPhysChem* **2010**, *11*, 999.
[24] G. Kervern, G. Pintacuda, Y. Zhang, E. Oldfield, C. Roukoss, E. Kuntz, E. Herdtweck, J.-M. Basset, S. Cadars, A. Lesage, C. Copéret, L. Emsley, *J. Am. Chem. Soc.* **2006**, *128*, 13545.
[25] C. F. Hwang, D. A. Hill, *Phys. Rev. Lett.* **1997**, *79*, 1011.
[26] K.-N. Hu, C. Song, H.-H. Yu, T. M. Swager, R. G. Griffin, *J. Chem. Phys.* **2008**, *128*, 052302.
[27] T. Maly, L. B. Andreas, A. A. Smith, R. G. Griffin, *Phys. Chem. Chem. Phys.* **2010**, *12*, 5872.
[28] M. Afeworki, J. Schaefer, *Macromolecules* **1992**, *25*, 4097.
[29] G. R. Khutsishvili, *Physics-Uspekhi* **1969**, *11*, 802.
[30] D. S. Wollan, *Phys. Rev. B* **1976**, *13*, 3671.
[31] U. Akbey, W. T. Franks, A. Linden, S. Lange, R. G. Griffin, B.-J. van Rossum, H. Oschkinat, *Angew. Chem.* **2010**, *122*, 7971; *Angew. Chem. Int. Ed.* **2010**, *49*, 7803.